

Comparison of 3 Compartment Kinetic Model and the Patlak Graphical Method for Calculating Ki from Dynamic FDG-Pet Images of a Mouse Heart *In Vivo*

Tanmay Chordia and
(telephone: 408-931-1044, tchordia@gmail.com)

Bijoy K. Kundu, PhD
Department of Radiology and Medical Imaging, University of Virginia, VA 22908 USA
(telephone: 434-924-0284, bkk5a@virginia.edu)

Introduction: Currently, the gold standard for measure the net influx of glucose into the tissue is catheter blood sampling, which yields an accurate measurement. However, the downside of this method is its intrusiveness making it less than ideal for situations in which the patient cannot be disturbed. The goal of this study is to compare the quantitative accuracy of the 3-compartment kinetic model and the graphical Patlak method for calculating the rate of [¹⁸F] fluoro-2deoxy-D-glucose (FDG) uptake, Ki, in the mouse brain unintrusively. The data for this calculation was derived from a previous PET scan on mice *in vivo*. We used both Cardiac gated and ungated images in this study. The applications of these models include early diagnosis of cancer by noting an increase in net glucose influx, which corresponds to a higher requirement of glucose to sustain the quick replication of cancerous cells.

Methods: Ki in mouse brain was first computed in a 3-compartment kinetic model (**Figure 1**).

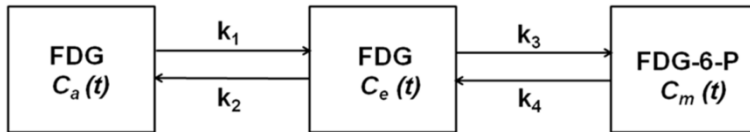


Figure 1: 3-compartment kinetic model

Based on this model the FDG concentration in the brain tissue can be written as follows:

Eq 1.

$$C_T(t) = \frac{K_1}{\alpha_2 - \alpha_1} \times [(K_3 + K_4 - \alpha_1)e^{-\alpha_1 t} + (\alpha_2 - K_3 - K_4)e^{-\alpha_2 t}] \otimes C_A(t) + BV C_A(t)$$

where

$$\alpha_{2,1} = 1/2(K_2 + K_3 + K_4 \pm \sqrt{(K_2 + K_3 + K_4)^2 - 4K_2K_4}),$$

\otimes is the convolution operator. K_1 and k_2 are the forward and reverse rate constants respectively between the first 2 compartments, k_3 and k_4 are the rates of phosphorylation and de-phosphorylation between compartments 2 and 3. BV is the fraction of the blood in the tissue modeling the spill-out of FDG from the blood into tissue at the early time points in a dynamic

FDG PET scan. This spill out occurs due to the limited intrinsic spatial resolution of the PET scan which results in some

The input function, $C_A(t)$, was measured by drawing regions of interest (ROI) in the left ventricular blood pool of the last frame of the dynamic FDG PET image of the mouse heart at end-diastole using ASIPro (Siemens Inc).³ 3 ROIs were taken in separate slices of the image and averaged out to obtain the function. The left ventricle blood pool was chosen because the large volume of blood minimizes spillover. The tissue time activity curve, $C_T(t)$, was obtained by drawing regions of interest on the same images in the region corresponding to the mouse brain, as shown in **Figure 2**.

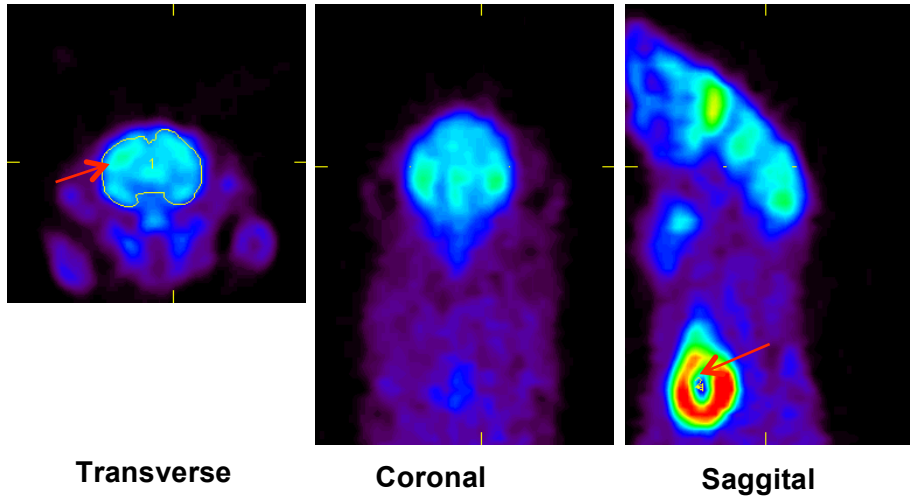


Figure 2: Example FDG PET images of mouse brain (red arrow in transverse image) and heart (red arrow in saggital image).

The rate constants from equation 1, obtained by non-linear regression (written in Matlab), were used to compute K_i as follows:

Eq 2.

$$K_i(\text{ml blood} \cdot \text{ml lung}^{-1} \cdot \text{min}^{-1}) = K_1 \frac{K_3}{(K_2 + K_3)}$$

K_i was also computed using the graphical Patlak method(also written in Matlab, using linear regression on the following formula, where K_i is the slope of the line:

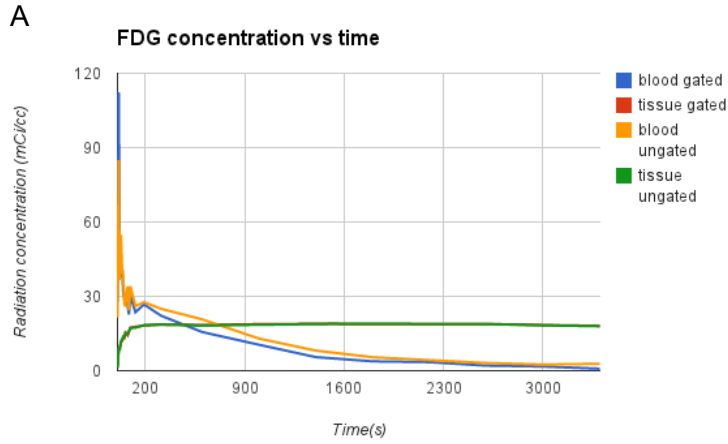
Eq 3.

$$\frac{C_T(t)}{C_A(t)} = K_i \times \frac{\int_0^t C_A(\tau) d\tau}{C_A(t)} + \text{Int}$$

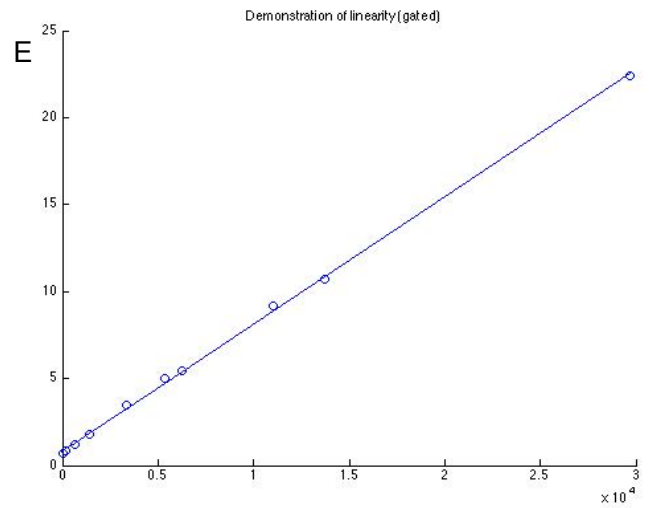
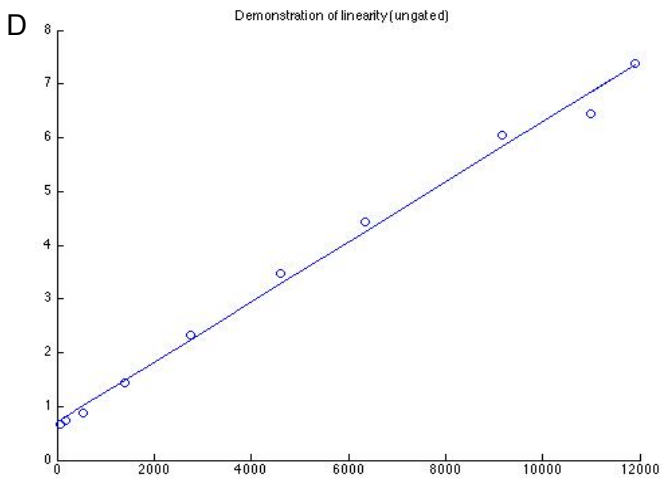
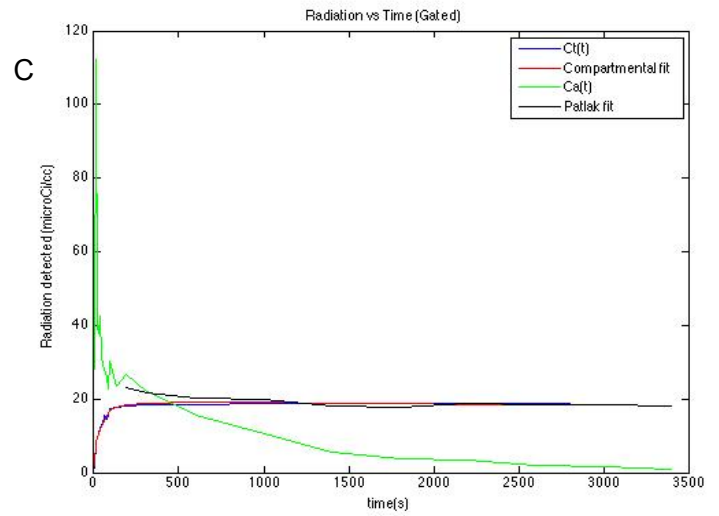
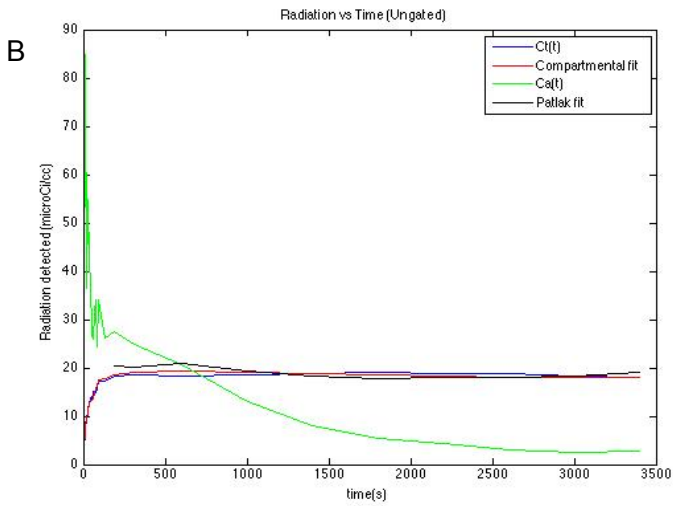
Results:

Figure 4 A) Shows the relationship between the cardiac gated and ungated images. Both $C_a(t)$ input functions are quite close. **B)** Demonstrates the fit to the $C_t(t)$ tissue curve with ungated images, while **C)** demonstrates the fit with gated images. For **B** and **C** The green line is $C_a(t)$,

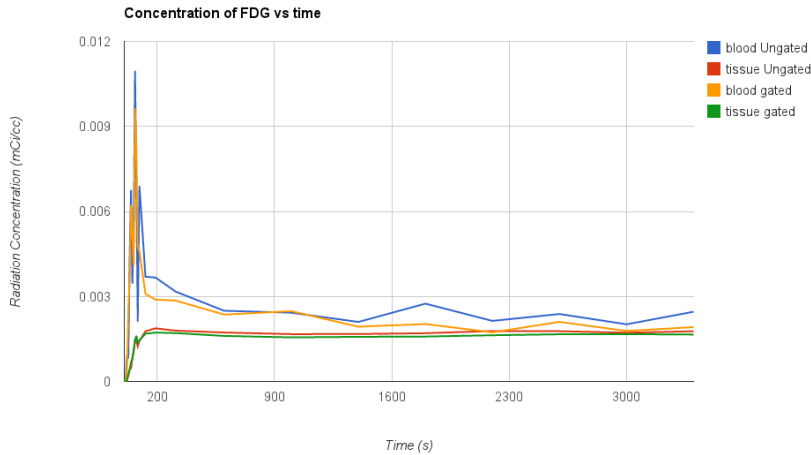
the blood input function, the blue line is $C_t(t)$, the tissue input function, the red line is the compartmental modelling fit, and the black line is the Patlak fit. Images of the first mouse sample are labelled **1** while the second mouse sample are labelled **2**.



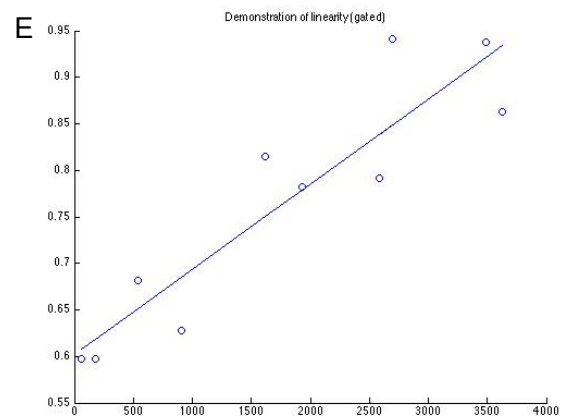
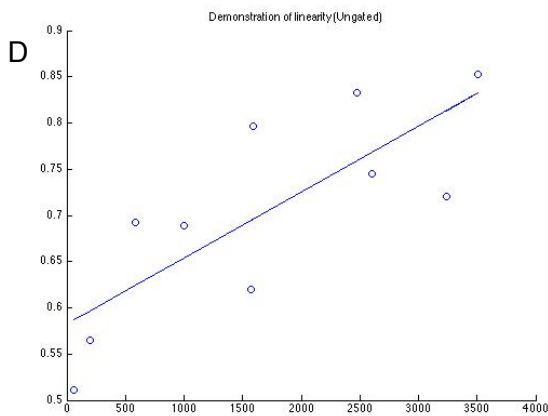
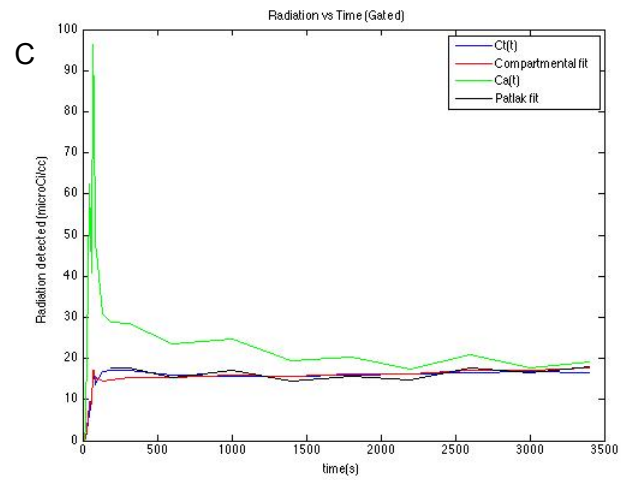
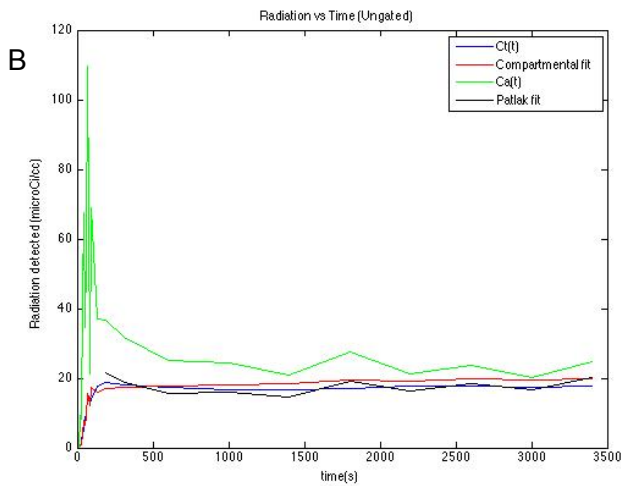
The gated $C_a(t)$ input function peaks higher than the ungated one, and dips slightly lower. This graph shows that there is only a small improvement made by cardiac gating. On the other hand, there is definitely an improvement. In addition, because the heart contractions are gated, gating has no effect on the $C_t(t)$ tissue function.



The above demonstrates the fit between the parameters and the observed input function. **B** and **C** show the Compartmental and Patlak fit overlaying the input function values. The Compartment model fits the entire $C_t(t)$ curve, and gives values for all 4 k constants and the BV component. When employing gated Compartmental modelling of this image, $k_1 = .029$, while $k_1 = 0.0824$, $k_2 = 0.0368$, $k_3 = 0.020$, $k_4 = 0$, and $BV = 0.014$. When using ungated images, $k_1 = .031$, while k values were $k_1 = 0.0657$, $k_2 = 0.0239$, $k_3 = 0.0217$, $k_4 = 0$ and the $BV = 0.00496$. In addition, although the Patlak fit was fairly close, excluding the beginning time points, the values for k_i were not as accurate as the compartmental modelling fit. The k_i using Patlak was computed as 0.033 when gated, and 0.044 when ungated. The fit appears to be quite close in both images, but the K_i values are less precise. **D** and **E** confirm the linearity of **Eq. 3**, ensuring the feasibility of linear regression. There is some discrepancy in the literature, as the K_i value is reported as .029 and .024 by different researchers, but the Compartmental model appears to be more accurate.



The gated $Ca(t)$ input function actually peaks lower, but does decrease more during later data points. However, there appears to be significant spillover in this result, as the blood function does not drop below the tissue function.



2 shows the second trial with different data. All of the fits appear to be close but slightly off. Here, the Compartment model once again fits the entire $Ct(t)$ curve, and gives values for all 4 k constants and the BV component. The model yields the following values: $k_1 = .025$, while $k_1 = 0.0858$, $k_2 = 0.0299$, $k_3 = 0.023$, $k_4 = 0$, and $BV = 0.00411$. For ungated images, $k_1 = .031$, while k values were $k_1 = 0.0674$, $k_2 = 0.0249$, $k_3 = 0.0301$, $k_4 = 0$ and the $BV = 0.00393$. Once again, the compartmental model fit was significantly better than the Patlak model. The k_i using Patlak was

computed as 0.039 when gated, and 0.047 when gated. The fit appears to be quite close in both images, but the K_i values are less precise. Once again, **D** and **E** confirm the linearity of **Eq. 3**. The fit appears to be much weaker in this instance, which explains the unusually high K_i values. This tim

Conclusions:

The results showed that the 3 compartment kinetic model was slightly more accurate in determining the net influx, with an average 2.7% error as opposed to the Patlak method with an average 3.9% error, which was attributed to the tighter fit of the kinetic model to the Time Activity Curves of the radiation concentration in the tissue and the blood. The compartmental model was quite accurate, and thus can be confirmed as the superior non-intrusive method of estimating K_i . This method has applications in diagnosing cancer early by locating cancerous tissue in the brain by the increase in the K_i constant due to the increased sugar necessary for runaway cancerous replication.

Reference List

- (1) Krivokapich J, Huang SC, Phelps ME et al. Estimation of rabbit myocardial metabolic rate for glucose using fluorodeoxyglucose. *Am J Physiol* 1982 December;243(6):H884-H895.
- (2) Patlak CS, Blasberg RG. Graphical Evaluation of Blood-To-Brain Transfer Constants from Multiple-Time Uptake Data - Generalizations. *Journal of Cerebral Blood Flow and Metabolism* 1985;5(4):584-90.
- (3) Locke LW, Berr SS, Kundu BK. Image-Derived Input Function from Cardiac Gated Maximum a Posteriori Reconstructed PET Images in Mice. *Mol Imaging Biol* 2011 April;13(2):342-7.